Invited Paper

Progress on large-area polarization grating fabrication

Matthew N. Miskiewicz, Jihwan Kim, Yanming Li, Ravi K. Komanduri and Michael J. Escuti

North Carolina State Univ, Dept Electrical & Computer Engineering, Raleigh, NC (USA)

ABSTRACT

Over the last several years, we have pioneered liquid crystal polarization gratings (PGs), in both switchable and polymer versions. We have also introduced their use in many applications, including mechanical/non-mechanical laser beam steering and polarization imaging/sensing. Until now, conventional holographic configurations were used to create PGs where the diameter of the active area was limited to 1-2 inches. In this paper, we discuss a new holography setup to fabricate large area PGs using spherical waves as the diverging coherent beams. Various design parameters of this setup are examined for impact on the quality of the recorded PG profile. Using this setup, we demonstrate a large area polymer PG with approximately 6×6 inch square area, and present detailed characterization.

Keywords: polarization gratings, holography, liquid crystal, polymer, diffraction

1. BACKGROUND

Polarization Gratings (PGs) are diffractive thin-film elements which act as polarizing beam splitters.[1–4] They have been used in a variety of applications such as polarization imaging systems, displays, and beam steering systems.[5–10] We have in the past proposed a number of designs for beam steering systems utilizing polarization gratings, resulting in high-efficiency, low-cost, compact steerers.[11–15] However, for reasons soon to be discussed, fabrication of PGs has been limited to samples with diameters in the range of $1-2$ inches. This is sufficient for many applications, but large area PGs would present a number of benefits in various cases. For example in directed energy applications, larger PGs lead to a higher maximum power throughput, and in communications applications they enable larger antenna apertures.

PGs are fabricated using polarization holography, which entails the interference of beams of different polarizations to create a desired polarization profile. Because of this, in traditional setups for PG fabrication the dimensions of the optics must scale with the final dimensions of the PG. Thus, one of the primary obstacles in traditional setups for fabricating large area PGs is the need for equally large optics to create and redirect the recording beams. However, in this paper we describe an alternative fabrication method using diverging beams where the required size of the optics do not scale with the final PG dimensions. This allows large area PGs to be made in a low-cost, efficient manner that is similar to prior methods. We experimentally demonstrate this new method and provide detailed characterization of a large area PG.

It is worthwhile to review the common prior holography setups used to create PGs. To create a PG, the polarization profile pattern shown in Fig. 1(a) must be created, which can be achieved by interfering two orthogonally circular beams. The interference profile has constant intensity and is linearly polarized; the polarization angle rotates in the x-dimension creating the grating. The classic approach to accomplish this includes lenses to expand and collimate an input laser beam, and involves sending the beam through a polarizing beam splitter (BS) and then a pair of quarter-wave plates (QWP) to create right and left circular beams as shown in Fig. 1(b). The beams are then redirected using mirrors (M) to interfere on the sample at a specific angle. The pitch of the PG is determined by the angle between the beams (the recording angle), and this angle can be controlled by adjusting the redirecting mirrors. This setup is very flexible, but also requires a large footprint, is sensitive to vibrations, and requires the tuning of various optics to change the pitch.

Correspondence should be sent to: mjescuti@ncsu.edu, Telephone: +1 919 513 7363

Acquisition, Tracking, Pointing, and Laser Systems Technologies XXVI,
edited by William E. Thompson, Paul F. McManamon, Proc. of SPIE Vol. 8395, 83950G
© 2012 SPIE · CCC code: 0277-786X/12/$18 · doi: 10.1117/12.921572

Downloaded from SPIE Digital Library on 30 May 2012 to 152.14.242.113. Terms of Use: http://spiedl.org/terms

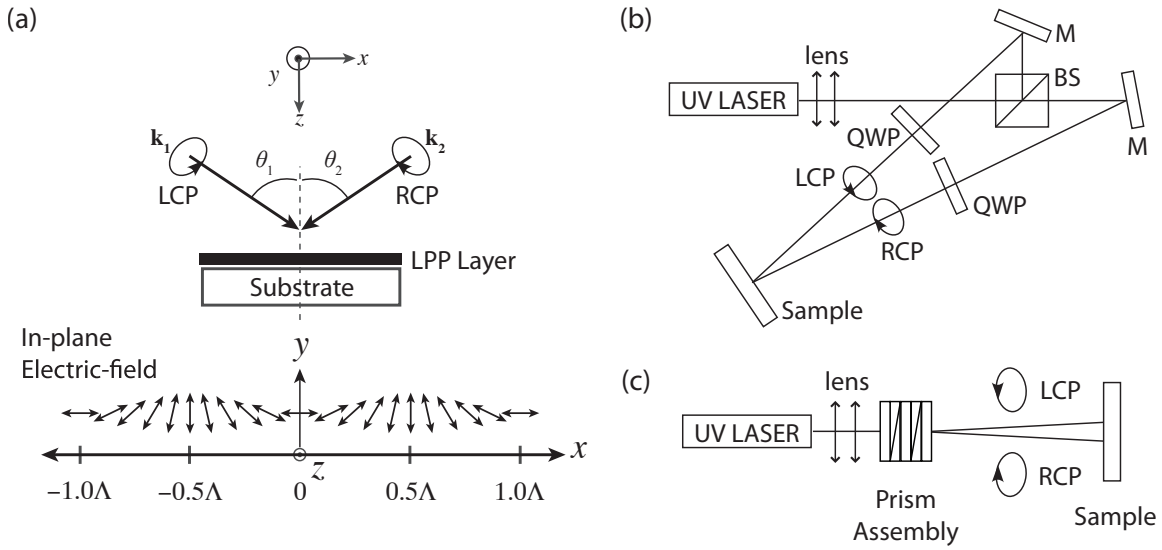

Figure 1: (a) PG profile created as an interference pattern from two orthogonally circularly polarized beams: RCP (Right-handed Circular Polarization); LCP (Left-handed Circular Polarization). (b) A layout of classic holography setup to create a PG. (c) A layout of proposed holography setup based on two rotating prisms.[16]

A recent publication describes a different approach which we call the birefringent prism setup[16] (Fig. 1(c)). This setup does not use a polarizing beam splitter or redirecting mirrors, but instead utilizes a pair of Wollaston prisms and some waveplates to create two beams, set their polarization, and set the recording angle. The recording angle is adjusted by rotating one of the Wollaston prisms. This setup has the advantages over the classic setup of being compact, requiring fewer optics, and being less sensitive to vibrations. It is also very easy to change the pitch compared the classic setup. For these reasons, our holography setup for large area PGs will be based on the birefringent prism setup.

2. HOLOGRAPHY SETUP

Fig. 2 shows the holography setup used to make large area PGs. The setup is a variation on the birefringent prism setup; instead of a lens to collimate the beam after the spatial filter, the lens is used to diverge beam a desired amount. The diverging beam passes through the Wollaston prism and waveplates and arrives at the sample, at which point the beam has expanded to fill the desired aperture. We have solved the problem of having a small aperture, but have introduced a new problem: the interference of two diverging beams is more complex than that of collimated beams. The resulting polarization interference pattern is similar to Fig. 1(a), but the grating pitch varies spatially across the sample. For a target pitch of Λ_0 where Λ_{edge} is the pitch at the edge of the desired aperture, we define the maximum relative variation in pitch over the sample as

$$\delta = \frac{\Lambda_{edge} - \Lambda_0}{\Lambda_0}. \tag{1}$$

To find the resulting interference pattern and thus δ, we will model the setup using two interfering spherical waves. The waves are assume to be identical but centered at different points on the x-axis and the sample is placed a distance L along the z-axis. Considering only the optical path differences between the beams in the x-dimension, we find

$$\Lambda(x) = \frac{\lambda}{\frac{x+x_0}{\sqrt{(x_0+x)^2+z_0^2}} - \frac{x-x_0}{\sqrt{(x-x_0)^2+z_0^2}}}, \tag{2}$$

Downloaded from SPIE Digital Library on 30 May 2012 to 152.14.242.113. Terms of Use: http://spiedl.org/terms

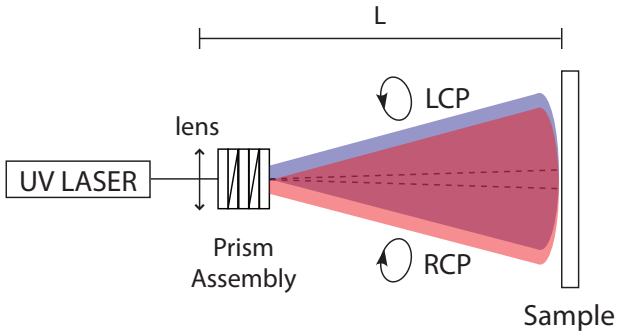

Figure 2: The holography setup used in this paper to fabricate large area PGs. The prism assembly consists of a QWP, Wollaston prism, HWP, Wollaston prism, then QWP.

where x is a point along the sample and $2x_0$ is the distance between the center of the spherical waves. In a purely spherical wave scenario, z would be equal to the distance from the sample plane from the source beams; however, to make use of diverging gaussian waves, will make this substitution

$$z_0 = R = l + L + \frac{z_R^2}{l + L}, \tag{3}$$

where l is the distance from the beam waist to the lens, L is distance from the lens to the sample (the throw distance), and z_R is the Rayleigh range.[17] Defining additional terms for wavelength λ, beam waist w_0, divergence θ, the radius of the beam entering the lens a_0, and the radius of the desired exposure area a_s, we can write the following equations

$$x_0 = \frac{R}{2\sqrt{(\Lambda_0/\lambda)^2 - 0.25}} \tag{4}$$

$$z_R = \pi/\lambda * w_0^2 \tag{5}$$

$$l = \frac{\pi w_0}{\lambda}\sqrt{a_0^2 - w_0^2} \tag{6}$$

$$\theta = \frac{\lambda}{\pi w_0} \tag{7}$$

$$\Lambda_{edge} = \Lambda(x = a_s). \tag{8}$$

For some Λ_0, a_0, and a_s and using Eqs. 2-8, we can solve for δ in terms of L and θ. The equation is long and not very informative, so we will instead plot some representative cases in order to understand how δ behaves. From Fig. 3, we see that lower throw distances result in higher δ. In addition, larger a_s/a_0 ratios increase δ. The important insight to be had is that in order to achieve low δ, a large throw distance is required. Choosing too small of a throw distance will result is substantial pitch variation across the sample.

Lastly, our experiments indicate that this theoretical model breaks down if Λ_0 is very large, on the order of 100 μm or larger. At those scales, secondary effects such as path-length differences between beams, wavefront variations, and the reality of gaussians waves instead of spherical ones play a dominant role, and so a more complete model is required to predict $\Lambda(x)$.

Downloaded from SPIE Digital Library on 30 May 2012 to 152.14.242.113. Terms of Use: http://spiedl.org/terms

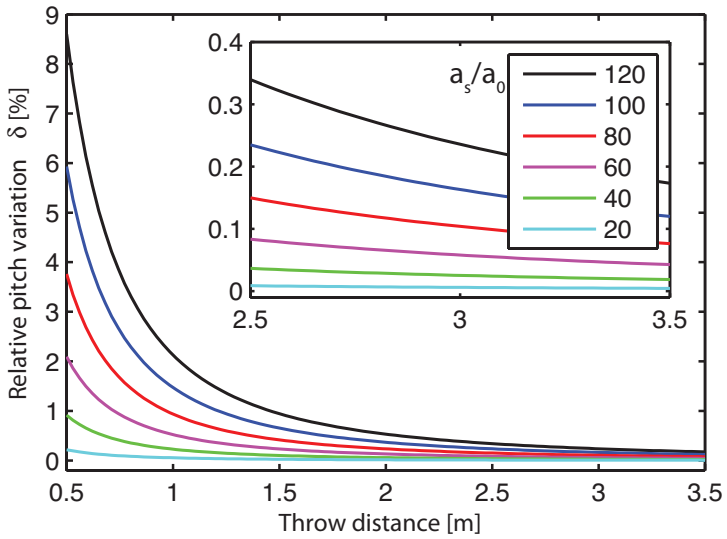

Figure 3: The curves show the relationship between δ and L for various a_s/a_0 ratios. The divergence θ is chosen so that the beam size at the sample equals a_s; Inset: a close up of the curves around $L = 3$ m.

3. EXPERIMENT

Using the holography setup and theory presented in Section 2, we fabricated a large area PG. The design was for a narrowband, passive (polymer) PG with a grating pitch of 5.8 μm (diffraction angle 10°) and half-wave retardation in the NIR range. The aperture of the PG was 6×6 inch square, roughly 22 cm diameter. The aperture of the input beam was 2 mm in diameter and we used a throw distance of 3 m.

The sample was first coated with a photo-alignment layer, DIC: LIA-C001, and was then exposed using a 355 nm laser with an exposure energy of about 0.1 J/cm^2. We have found vibrations to be one of the main causes of failed samples. To limit their effect, we employ a standard air-damped optics table with an enclosure to prevent perturbations from air currents. The sample mounting is also critical; mounting the sample insecurely or in certain types of holders will almost always fail. We mounted the sample vertically and created the PG but the sample could be mounted horizontally as well with a 45° turning mirror to redirect the recording beam.

After exposure, a liquid crystal (LC) layer using the reactive mesogen RMS10-025 (Merck, $\Delta n = 0.16$) was spin-coated on top of the exposed photo-alignment layer. Four layers were spun to bring the retardation to half-wave at 1130 nm, each layer being polymerized with a UV lamp. The first layer was 1:3 RMS10-025:PGMEA and was spun for 30 seconds at 1500 rpm/s. The second, third, and fourth layers were undiluted RMS10-025 spun for 45 seconds at 700 rpm/s. By slightly adjusting the recipe, the thickness can be tuned for any desired half-wave thickness.

4. RESULTS

Qualitatively, the sample was a success and functioned as expected. Because the wavelength is tuned for the NIR, there is a maxima in zero-order transmittance around red wavelengths and a minima around blue wavelengths (Fig. 4(b)). This can produce some striking images when looking through the PG, as depicted in Fig. 4(a). A view of the grating between crossed polarizers is also shown in Fig. 4(b), from which we can qualitatively see good alignment, low defect density, and no discernible variation in pitch.

The sample has been characterized in a number of ways to quantify its performance. The first parameter quantified is the grating pitch uniformity. The theory from above predicts a δ of 0.18% which translates to a maximum variation of 0.01 μm or 0.02° at the design wavelength. We measured the maximum variation to be 0.01 μm, matching the expected value. It should be emphasized that this low of a δ is not guaranteed with this setup; we obtained it by choosing sufficiently low θ and high L.

Downloaded from SPIE Digital Library on 30 May 2012 to 152.14.242.113. Terms of Use: http://spiedl.org/terms

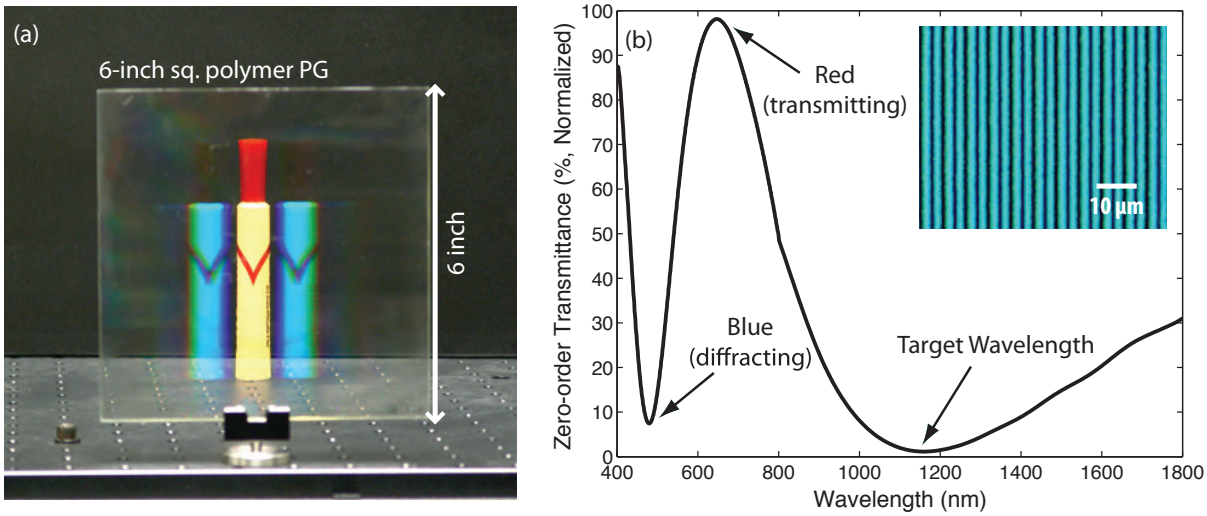

Figure 4: (a) A white maker with a red cap as seen through the PG, (b) The zero-order transmittance spectrum explains the view of the marker: red light is transmitted through the PG without diffracting, while blue light is largely diffracted. Inset: the PG viewed through crossed polarizers.

To measure the uniformity of the LC thickness, we can measure the uniformity of the half-wave wavelength over the sample, obtainable from the spectrum of the zero order transmittance. Fig. 5 shows the zero order transmittance spectrum for 9 regions on the sample (see the inset of the Fig. 5). Table 1 shows the half-wave wavelengths in these regions, from which we calculate a thickness uniformity of 96%. The non-uniform thickness is related to our spin coating process, which is not yet fully optimal for achieving very uniform films on large area substrates.

The first order diffraction efficiency of the sample was measured to be ~96% at 1064nm for all regions. The amount of scattering, defined as the percent light that does not go into the -1st, +1st, or orders was found to be

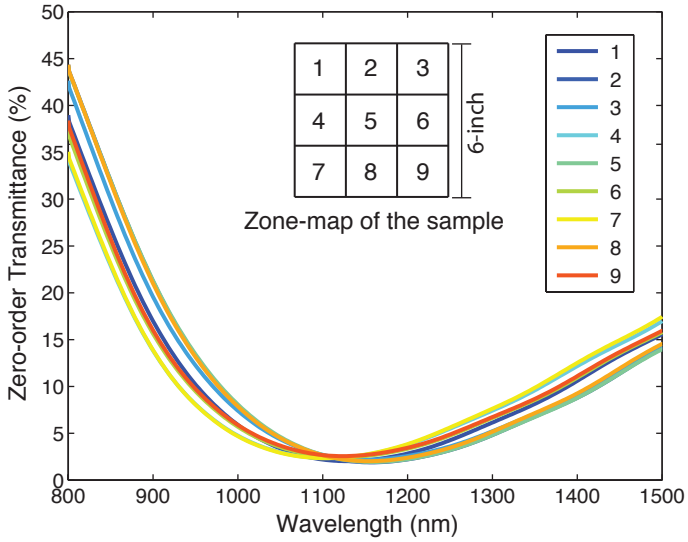

Figure 5: The zero-order transmittance spectrum measured in different regions of the sample. The curves have roughly the same minimum values, indicating equal alignment and diffraction efficiency, but differ in the location of the minima, indicating different thicknesses.

Downloaded from SPIE Digital Library on 30 May 2012 to 152.14.242.113. Terms of Use: http://spiedl.org/terms

1132	1152	1143
1110	1152	1126
1110	1150	1128

Table 1: Half-wave retardation wavelengths (nm) for different regions of the sample.

1.6% for all regions. The diffraction efficiency of this sample is somewhat sub-optimal, however, we believe that as with smaller PG samples, careful tuning of the spin coating recipe can eliminate the scattering and improve alignment to achieve >99% efficiency into a single order.

5. CONCLUSIONS

We have presented a new holography setup for fabricating large area PGs based on a birefringent prism setup, in combination with diverging beams at the plane of interference. The resulting polarization profile (and therefore grating pitch) is non-uniform and depends on a variety of parameters, and we presented equations to predict how the grating pitch will vary. We then fabricated a 6×6 inch PG using this new diverging beam birefringent prism setup. The sample's uniformity was characterized in terms of grating pitch, coating thickness, diffraction efficiency, and scattering. While some variations were present, the sample was of good quality over most of the entire aperture. To our knowledge this is the largest PG ever fabricated, and we expect this technology to lead to new and superior systems in the beam-steering field.

ACKNOWLEDGMENTS

The authors gratefully acknowledge the support of the National Science Foundation (NSF grant ECCS-0955127) and ImagineOptix Corp for this work.

REFERENCES

[1] Nikolova, L. and Todorov, T., "Diffraction efficiency and selectivity of polarization holographic recording," *Optica Acta* **31**(5), 579–588 (1984).

[2] Gori, F., "Measuring stokes parameters by means of a polarization grating," *Opt. Lett.* **24**(9), 584–586 (1999).

[3] Crawford, G. P., Eakin, J. N., Radcliffe, M. D., Callan-Jones, A., and Pelcovits, R. A., "Liquid-crystal diffraction gratings using polarization holography alignment techniques," *Journal of Applied Physics* **98**(12), 123102 (2005).

[4] Escuti, M. J., Oh, C., Sanchez, C., Bastiaansen, C., and Broer, D. J., "Simplified spectropolarimetry using reactive mesogen polarization gratings," *Proc. SPIE* **6302**, 630207 (2006).

[5] Jones, W. M., Conover, B. L., and Escuti, M. J., "Evaluation of projection schemes for the liquid crystal polarization grating operating on unpolarized light," *SID Symposium Digest* **37**, 1015–1018 (2006).

[6] Nersisyan, S. R., Tabiryan, N. V., Hoke, L., Steeves, D. M., and Kimball, B. R., "Polarization insensitive imaging through polarization gratings," *Opt. Express* **17**, 1817–1830 (2009).

[7] Nersisyan, S. R., Tabiryan, N. V., Steeves, D. M., and Kimball, B. R., "The principles of laser beam control with polarization gratings introduced as diffractive waveplates," *Proc. SPIE* **7775**, 77750U (2010).

[8] Kim, J. and Escuti, M. J., "Demonstration of a polarization grating imaging spectropolarimeter (pgis)," *Proc. SPIE* **7672**, 767208 (2010).

[9] Kudenov, M., Escuti, M. J., Dereniak, E., and Oka, K., "White light channeled imaging polarimeter using broadband polarization gratings," *Appl. Opt.* **50**, 2283–2293 (2011).

[10] Seo, E., Kee, H. C., Kim, Y., Jeong, S., Choi, H., Lee, S., Kim, J., Komanduri, R. K., and Escuti, M. J., "Polarization conversion system using a polymer polarization grating," *SID Symposium Digest* **42**, 540–543 (2011).

[11] Kim, J., Oh, C., Escuti, M. J., Hosting, L., and Serati, S., "Wide-angle, nonmechanical beam steering using thin liquid crystal polarization gratings," *Proc. SPIE* **7093**, 709302 (2008).

Downloaded from SPIE Digital Library on 30 May 2012 to 152.14.242.113. Terms of Use: http://spiedl.org/terms

[12] Oh, C., Kim, J., Muth, J. F., Serati, S., and Escuti, M. J., "High-throughput, continuous beam steering using rotating polarization gratings," *IEEE Phot. Tech. Lett.* **22**, 200–202 (2010).
[13] Kim, J., Miskiewicz, M. N., Serati, S., and Escuti, M. J., "High-efficiency quasi-ternary design for nonmechanical beam-steering utilizing polarization gratings," *Proc. SPIE* **7816**, 78160G (2010).
[14] Kim, J., Oh, C., Serati, S., and Escuti, M. J., "Wide-angle, nonmechanical beam steering with high throughput utilizing polarization gratings," *App. Opt.* **50**(17), 2636–2639 (2011).
[15] Kim, J., Miskiewicz, M. N., Serati, S., and Escuti, M. J., "Demonstration of large-angle nonmechanical laser beam steering based on lc polymer polarization gratings," *Proc. SPIE* **8052**, 80520T (2011).
[16] Kim, J., Komanduri, R. K., and Escuti, M. J., "A compact holographic recording setup for tuning pitch using polarizing prisms," *Proc. SPIE* **8281**, 82810R (2012).
[17] Hecht, E., [*Optics*], Addison-Wesley Pub. Co., San Francisco, 4th ed. (2002).

Downloaded from SPIE Digital Library on 30 May 2012 to 152.14.242.113. Terms of Use: http://spiedl.org/terms